

12

AD-A230 221

Microphase-Separation Interpretation of the Covariation of Several Polyurethane Dielectric Properties

Prepared by

R. S. BRETZLAFF and R. Y. SUGIHARA
Materials Sciences Laboratory
Laboratory Operations

DTIC
ELECTE
DEC 20 1990
S D

28 September 1990

Prepared for

SPACE SYSTEMS DIVISION
AIR FORCE SYSTEMS COMMAND
Los Angeles Air Force Base
P.O. Box 92960
Los Angeles, Ca 90009-2960

Co

Development Group


THE AEROSPACE CORPORATION
El Segundo, California

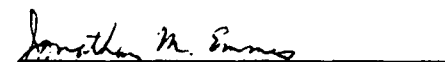
UNCLASSIFIED BY 6032/ML/A
DATE 08-11-2001

This report was submitted by The Aerospace Corporation, El Segundo, CA 90245, under Contract No. F04701-88-C-0089 with the Space Systems Division, P.O. Box 92960, Los Angeles, CA 90009-2960. It was reviewed and approved for The Aerospace Corporation by S. Feuerstein, Director, Materials Sciences Laboratory. Captain Andrew Chrostowski was the Air Force project officer for the Mission-Oriented Investigation and Experimentation (MOIE) program.

This report has been reviewed by the Public Affairs Office (PAS) and is releasable to the National Technical Information Service (NTIS). At NTIS, it will be available to the general public, including foreign nationals.

This technical report has been reviewed and is approved for publication. Publication of this report does not constitute Air Force approval of the report's findings or conclusions. It is published only for the exchange and stimulation of ideas.


ANDREW CHROSTOWSKI, Capt, USAF
MOIE Project Officer
SSD/MSSM


JONATHAN M. EMMES, Maj, USAF
MOIE Program Manager
AFSTC/WCO OL-AB

REPORT DOCUMENTATION PAGE

1a. REPORT SECURITY CLASSIFICATION Unclassified		1b. RESTRICTIVE MARKINGS	
2a. SECURITY CLASSIFICATION AUTHORITY		3. DISTRIBUTION/AVAILABILITY OF REPORT Approved for public release; distribution is unlimited.	
2b. DECLASSIFICATION/DOWNGRADING SCHEDULE			
4. PERFORMING ORGANIZATION REPORT NUMBER(S) TR-0089(4935-03)-1		5. MONITORING ORGANIZATION REPORT NUMBER(S) SSD-TR-90-36	
6a. NAME OF PERFORMING ORGANIZATION The Aerospace Corporation Laboratory Operations	6b. OFFICE SYMBOL (if applicable)	7a. NAME OF MONITORING ORGANIZATION Space Systems Division.	
6c. ADDRESS (City, State, and ZIP Code) El Segundo, CA 90245-4691		7b. ADDRESS (City, State, and ZIP Code) Los Angeles Air Force Base Los Angeles, CA 90009-2960	
8a. NAME OF FUNDING/SPONSORING ORGANIZATION	8b. OFFICE SYMBOL (if applicable)	9. PROCUREMENT INSTRUMENT IDENTIFICATION NUMBER F04701-88-C-0089	
8c. ADDRESS (City, State, and ZIP Code)		10. SOURCE OF FUNDING NUMBERS	
		PROGRAM ELEMENT NO.	PROJECT NO.
		TASK NO.	WORK UNIT ACCESSION NO.
11. TITLE (Include Security Classification) Microphase-Separation Interpretation of the Covariation of Several Polyurethane Dielectric Properties			
12. PERSONAL AUTHOR(S) Bretzlaff, Robert S. and Sugihara, Richard Y.			
13a. TYPE OF REPORT	13b. TIME COVERED FROM _____ TO _____	14. DATE OF REPORT (Year, Month, Day) 1990 September 28	15. PAGE COUNT 20
16. SUPPLEMENTARY NOTATION.			
17. COSATI CODES		18. SUBJECT TERMS (Continue on reverse if necessary and identify by block number)	
FIELD	GROUP	SUB-GROUP	
			Phase-Separated Polymers, → De Conductivity, Electrical
			Polyurethanes → Permittivity, Insulators
			Dielectric Breakdown Strength Dielectrics, Encapsulation
19. ABSTRACT (Continue on reverse if necessary and identify by block number)			
<p>Electronic power supplies, cables and other equipment depend upon the breakdown-free separation of charged conductors. This often requires the use of polymeric encapsulants or extruded dielectrics, whose thermal aging behavior is a concern. One high-voltage encapsulation is the polyurethane, Uralane 5853. It is composed of chain molecules based on (a) polybutadiene, existing in a long, flexible subchain (soft segments), and (b) methylene diisocyanate, existing in a short, rigid subchain (hard segments) linking the flexible subchains. The hard segments in different chains tend to form hydrogen bonds and to phase-separate. This work demonstrates the relation of Uralane's dielectric breakdown strength to its permittivity (50 Hz to 10 kHz) and to its dc conductivity, thereby illustrating an analytical technique for use in the formulation and evaluation of new polyurethanes. →</p> <p>Phase-separated polymer microstructures are hypothesized for force breakdown paths to assume more tortuous routes around electron-trap-rich, two-dimensional interphase boundaries, compared to polymers in which there are only "point defects" (free-volume holes and</p>			
20. DISTRIBUTION/AVAILABILITY OF ABSTRACT <input checked="" type="checkbox"/> UNCLASSIFIED/UNLIMITED <input type="checkbox"/> SAME AS RPT. <input type="checkbox"/> DTIC USERS		21. ABSTRACT SECURITY CLASSIFICATION Unclassified	
22a. NAME OF RESPONSIBLE INDIVIDUAL		22b. TELEPHONE (Include Area Code)	22c. OFFICE SYMBOL

19. ABSTRACT (Continued)

crosslinks), thereby helping to increase the dielectric breakdown strength, to decrease the dc conductivity, and to alter the permittivity via interactions between the microstructural domains. To test this hypothesis, accelerated thermal aging of 60-mil Uralane slabs was performed at 120°C in air for 0.5 or 4.0 hr. There was an initial decrease, followed by a partial reordering, of the paracrystalline domains, as determined by Fourier transform infrared spectroscopy. Moisture-evolution analysis confirmed that the amount of water (less than 0.03% by weight) lost by the polymer during aging was too small to account for the observed changes in electrical properties.

It was found that the (partially reversible) reduction in paracrystalline domain size correlated with a decrease in dielectric breakdown strength during thermal aging. All other things being equal, increased phase separation leads to diminished leakage current through the dielectric, with fewer energetic electrons available to possibly initiate failure during electrical aging. Testing is in progress on a new series of polyurethanes in order to ascertain the optimum hard-segment composition for thermal-aging voltage stability. ←

CONTENTS

I. INTRODUCTION.....	5
II. EXPERIMENTAL METHOD.....	9
III. EXPERIMENTAL RESULTS.....	11
IV. SUMMARY AND CONCLUSION.....	21
REFERENCES.....	23

FIGURES

1.	Compressive load vs strain for 60-mil-thick discs of Uralane 5753 after aging at 120°C in air.....	12
2.	FTIR difference spectra for Uralane 5753 aged at 120°C in air for (a) 0.0 hr, (b) 0.5 hr, and (c) 4.0 hr.....	13
3.	(a) Current-voltage characteristic for unaged Uralane 5753, and (b) conductivity for unaged Uralane 5753.....	15
4.	(a) Current-voltage characteristic for Uralane 5753 aged for 0.5 hr at 120°C in air, and (b) conductivity for Uralane 5753.....	16
5.	(a) Current-voltage characteristic for Uralane 5753 aged for 4.0 hr at 120°C in air, and (b) conductivity for Uralane 5753.....	17
6.	Logarithm of the real part of the permittivity graphed against the logarithm of the frequency for unaged, 0.5-hr-aged, and 4.0-hr-aged Uralane 5753.....	19
7.	Conductivity of Uralane 5753 graphed against the real part of the permittivity at 1.0 kHz.....	19
8.	Nominal dielectric breakdown strength of Uralane 5753 graphed against the real part of its permittivity at 1.0 kHz.....	20



Accession For	
NTIS	ORNL
DTIC	TRB
Unannounced	U
Justification	
By _____	
Distribution /	
Availability Codes	
Dist	Avail and/or Special
A-1	

I. INTRODUCTION

Polyurethanes [such as Uralane 5753, based on methylene diisocyanate and polybutadiene, and PRC 1535, based on toluene diisocyanate and poly(tetramethylene oxide)] form phase-separated structures because of the hydrogen-bonding capability of the hard segments, which are rich in N-H and C=O groups. Dielectric relaxations have been studied^{1,2} in block copolymers which are also microphase-separated. If the constituent phases possess significantly different electrical parameters, then trapping of charge carriers at the interfacial boundaries occurs and leads to low-frequency dielectric dispersion phenomenon. This phenomenon in layered dielectrics was first investigated by Maxwell,³ was developed further by Wagner⁴ and by Sillars,⁵ and is referred to as the "MWS effect."

In block copolymers, the loss peaks from this MWS effect occur in the 10^{-2} to 10^{-4} Hz range when the temperature is between 30 and 60°C in styrene-butadiene-styrene tri-block copolymers and in butane diol terephthalate - poly(tetramethylene oxide terephthalate) copolymer.^{1,2} Higher frequency relaxations exist due to microbrownian motion in the soft phase, with loss peaks typically between 200° and 300°K at 1 kHz. Since the dipolar polarizability and relaxation time of the soft phase will be affected by the degree of physical crosslinking provided by the hard phase, the higher-frequency relaxation (1 kHz) is an indirect monitor of the existence of crystal/amorphous interfaces. It is known that molecular disorder at these interfaces is a prominent source of electronic traps in the material.⁶⁻⁸ Therefore, the kilohertz permittivity is expected to be a measure of the electronic trapping capability.

The efficiency of charge-trapping is obviously a key parameter for dielectrics. Since structural disorder, the basis for trap formation, includes crosslinks, free-volume holes, impurities, partial charges on chemical groups, and the disorder at the crystal/amorphous interface, there are many ways to trap electrons. However, two-dimensional surfaces arising

from phase separation are expected to provide a key feature of electron trapping, because these phase-boundary networks help prevent an uninterrupted electron path parallel to the applied field, thereby reducing the chances for an electron to acquire enough energy for impact ionization. In addition to limiting the high-energy fraction of electrons, the strong trapping limits the overall current, i.e., the dc conductivity. The capacity of the traps to bind injected charge near electrode protrusions is a critical feature of the field-limited space charge (FLSC) theory.⁹⁻¹³ These are the reasons for studying the microstructure-dependent interrelation of the permittivity, dc conductivity, and the dielectric breakdown strength.

Phase-separated polymer microstructures are hypothesized to force breakdown paths to assume more tortuous routes around trap-rich, two-dimensional interphase boundaries, compared to polymers in which there are only "point defects" (free volume holes and crosslinks). We expect that higher crystallinity and more finely divided domains lead to lower dc conductivity and to higher dielectric breakdown strength. The permittivity could increase or decrease because of multipole interactions between the microdomains.^{14,15}

Phase-separated polyurethanes offer an opportunity to test this hypothesis. For example, Fourier transform infrared (FTIR) spectroscopy can be applied to the microscopic analysis of polymer dielectrics.¹⁶ Spectra show that both bonded and free N-H stretching vibrations exist in Uralane 5753, indicative of the existence of both paracrystalline and amorphous regions.¹⁷⁻¹⁹ Consistent with this hypothesis, we show below that the dc conductivity in Uralane 5753 can easily vary by a factor of 2 when thermal annealing is used to alter the microstructure. Trap-rich phase boundaries in the polyurethane PRC 1535 are changed by thermal aging, and the nominal dielectric breakdown is reduced.¹⁹ A theory of phase growth was devised in order to explain observed infrared spectral variations.¹⁹

It is desired to make permittivity and conductivity measurements that reflect the degree of microphase separation and that correlate with the

FTIR results for the paracrystallinity. This report also shows the relation of the nominal dielectric breakdown strength to the other electrical parameters. This approach assumes that the microstructure can be varied by thermal aging at 120°C for up to 4.0 hr without the appearance of other effects that cause variations in the electrical properties under test. There are three possible competing effects during aging: (1) water desorption, (2) depolymerization, and (3) additional cure. To eliminate the first possibility, water evolution analysis was performed. The second and third possibilities were evaluated by mechanical tensile tests which would show effects of any gross degradation.

II. EXPERIMENTAL METHOD

Freshly cured, 60-mil-thick (nominal) slabs of Uralane 5753 were prepared from its components, which are based on polybutadiene and methylene diisocyanate. The material batches were GLL-017 (part A) and MM-056 (part B). The slabs were allowed to post-cure for 2 weeks before commencing thermal aging studies. The slabs were cured, stored, and tested under ambient laboratory conditions of temperature and humidity. The aging was done at 120°C in air for 0.5 or 4.0 hr. All tests were performed at room temperature.

The water content of the Uralane samples was monitored with a DuPont water evolution analyzer. Mechanical properties were determined on 2-in.-diameter discs of Uralane by using an Instron in the compression mode (1 in./min crosshead speed and a 200-lb load cell). FTIR difference spectra of the thermally aged specimens relative to their original state were obtained. Transmission spectra were obtained from small slices microtomed off the aged material.

Dc conductivity measurements were performed on 3.25-in.-diameter disks of the 60-mil Uralane. Disk-shaped brass electrodes and a guard ring were used, the smaller electrode being 2 in. in diameter. The applied voltage was between 0 and 500 V, corresponding to an electric field of from 0 to 3.3 kV/cm. The current was registered with a Keithly 610 C electrometer and was in the range of 1 to 10 pA (0.32 to 3.2 pA/cm²). The current rose monotonically, stabilized, and was recorded about 30 sec after each increase in voltage. Each sample was remounted and measured three times in order to verify that there were no nonreproducible contact problems.

The real part of the permittivity was measured from 50 Hz to 10 kHz by a noncontacting electrode technique previously described.²⁰⁻²² The two embedding fluids were air and vegetable oil. A General Radio 1615 A capacitance bridge was used in conjunction with a sample cell conforming to ASTM D-150.

The nominal dielectric breakdown strength, F_b , was measured according to ASTM D-149. The voltage is increased at 600 V/sec to breakdown. Flat sheets were tested which were about 60 mils thick and which extended beyond the cylindrical brass electrodes of 1-in. diameter. These readings are typically at least an order of magnitude lower than the intrinsic material property ($F_b^{(0)}$) made with recessed electrodes,²³⁻²⁵ encapsulated electrodes,²⁶ or injected electrodes.^{27,28} The value is reduced because pre-breakdown discharges occur in the Fluorinert embedding fluid near the intersection of the electrode edges and the sample. We plan to apply one of these methods in the future.

These experiments were performed in order to test the working hypothesis. As polymer microstructure becomes more finely divided, it can store more charge through interfacial polarization. The real part of the permittivity can increase or decrease, due to multipole interactions, as noted above.

III. EXPERIMENTAL RESULTS

The moisture evolution analyzer was calibrated with sodium tungstate (theoretical water content 10.92%). Sixty-minute heating times at 180°C were employed on all moisture analyzer tests. The result for sodium tungstate was 10.72%. The results for the unaged, 0.5-hr aged, and 4.0-hr aged Uralane were 0.040%, 0.036%, and 0.012%, respectively. The mechanical test results are shown in Fig. 1. There is no significant difference between the mechanical results.

The infrared survey spectrum shows a bonded N-H stretching resonance at 3327 cm^{-1} and shoulders corresponding to free N-H stretching at 3370 and 3423 cm^{-1} . The initial difference spectrum at time zero (Fig. 2a) is flat, as expected. After 0.5 hr of heating at 120°C in air, there is a pronounced decrease in absorbance at 3309 cm^{-1} (Fig 2b), corresponding to a decreased volume or perfection of paracrystalline regions. (The difference between 3309 and 3327 cm^{-1} is inconsequential in such a broad band, whose width reflects a wide range of intermolecular environments.) After 4.0 hr of aging (Fig. 2c), the 3309 cm^{-1} band has returned to zero absorbance, but there are small increases at 3354 and 3424 cm^{-1} . Evidently there are more hard segments "dissolved" in the soft phase, with N-H vibrations at the "free" (nonhydrogen bonded) resonant frequencies. Since we expect the total number of hard segments to be conserved, we must consistently infer that the average hard-domain absorptivity (per segment) must not be conserved. Our interpretation is that, between 0.5 and 4.0 hr, the paracrystals start to reorder (increasing their 3309 cm^{-1} absorbance) but without some of the segments that were originally present in the paracrystals. This latter change tends to decrease the 3309 cm^{-1} absorbance. The resulting change near 3309 cm^{-1} is zero. The increases near 3424 and 3354 cm^{-1} come from the hard segments that are "dissolved" in the soft phase as a result of the "shaking out" process which perfected the paracrystals.

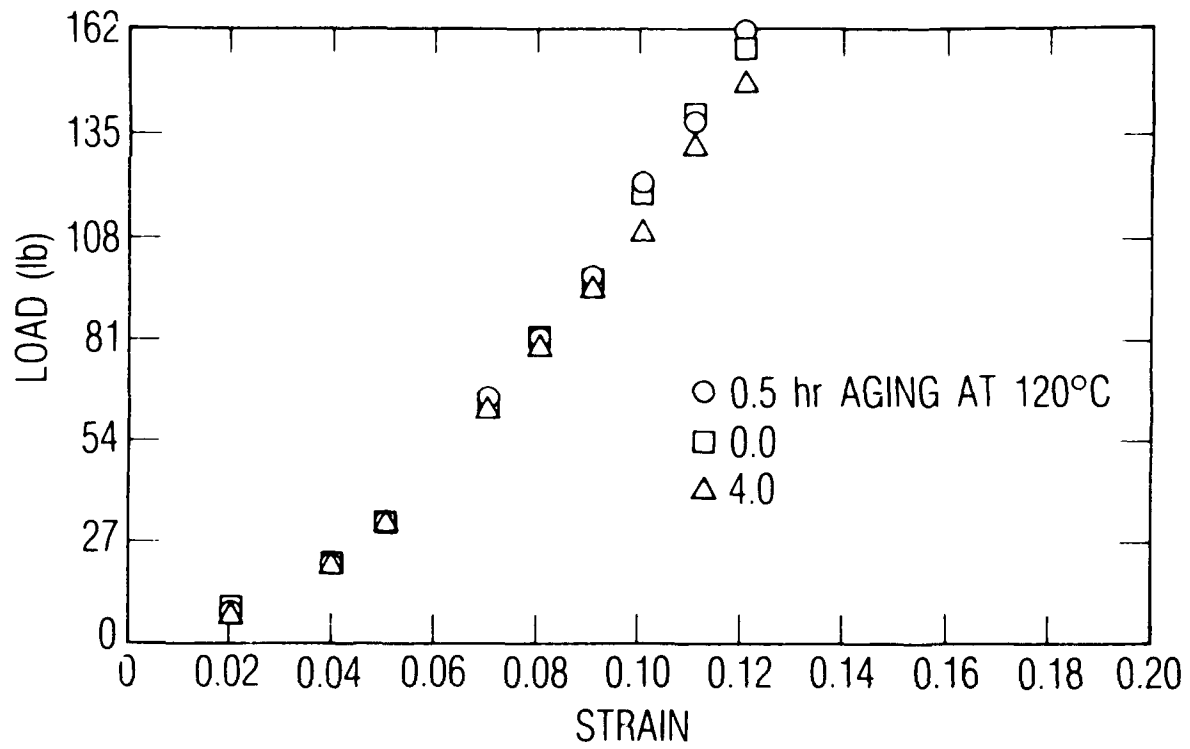


Fig. 1. Compressive load vs strain for 60-mil-thick discs of Uralane 5753 after aging at 120°C in air

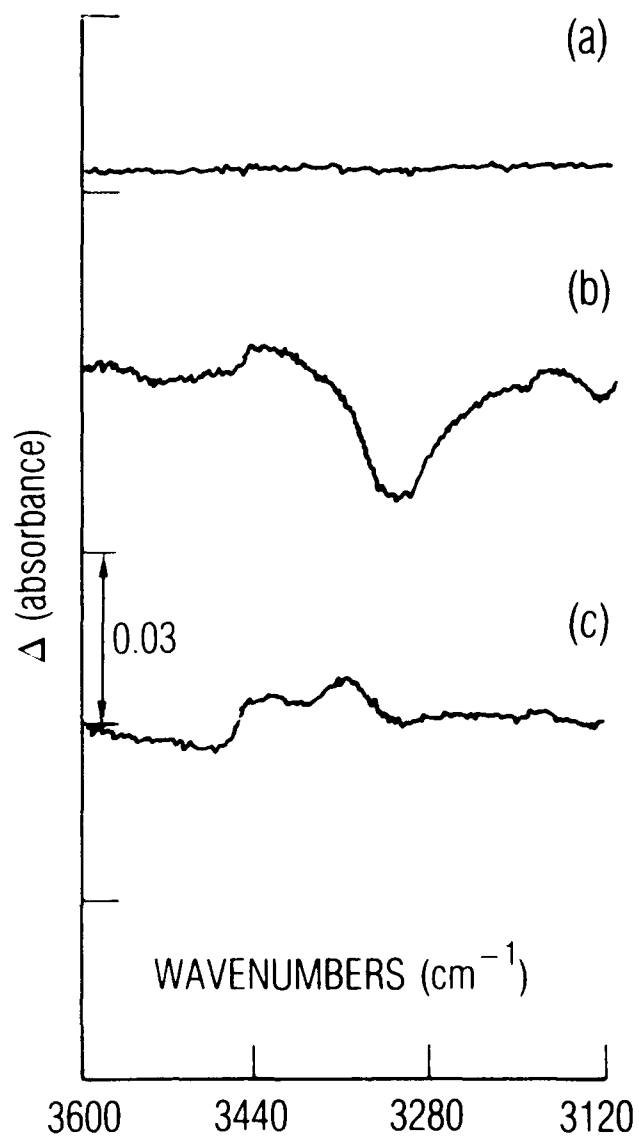


Fig. 2. FTIR difference spectra for Uralane 5753 aged at 120°C in air for (a) 0.0 hr, (b) 0.5 hr, and (c) 4.0 hr

Figure 3a shows the raw data points for three successive current-voltage measurements on the as-cast Uralane. It is noted that the currents range from 1 to 10 pA, the voltages from 0 to 500 V, the current density from 0.32 to 3.2 pA/cm², and the fields from 0 to 3.3 kV/cm. The solid curve in Fig. 3a is a least-squares curve fit to $I = aV + bV^2$. The curve is virtually linear (ohmic response). The conductivity is $\sigma(V) = (L/A) \cdot (dI/dV)$, where L is the sample thickness and A is the electrode area. There is a modest decrease (Fig. 3b) in the conductivity over the 0 to 500 V range. Apparently some of the trapping centers are more effective at the higher fields in this measurement. The zero-field conductivity is about 0.15 fempto mho/cm, in essential agreement with the manufacturer's specification of 0.11 fempto mho/cm.

Figure 4a shows the raw data points for the 0.5-hr, 120°C aged Uralane. The overall currents are higher, and now there is an appreciable nonohmic response. At zero voltage the conductivity has only increased from 0.147 to 0.165 fempto mho/cm. Over the entire 0 to 500 V range, however, the conductivity almost doubles (Fig. 4b), in sharp contrast to Fig. 5b. This behavior is consistent with the working hypothesis that there are fewer paracrystalline regions, fewer traps, and a less inhibited current flow in this thermally aged sample.

Figures 5a and 5b (at 4.0 hr) show that the current and conductivity have subsided from their values in Figs. 4a and 4b (at 0.5 hr), although both quantities are still uniformly higher than in the unaged sample. This is consistent with the FTIR results: The paracrystalline regions have been largely restored, but with some of the hard segments now "dissolved" in the soft phase. If the absorptivity (per segment) is assumed to have gone up in order to achieve the flat response at 3309 cm⁻¹, then the paracrystals would evidently be more perfect. So while there are more paracrystals, interfaces, and electron traps in the 4.0-hr aged sample compared to the 0.5-hr aged one, the paracrystals are more perfect, and there are fewer traps in the 4.0-hr aged sample compared to the initial state.

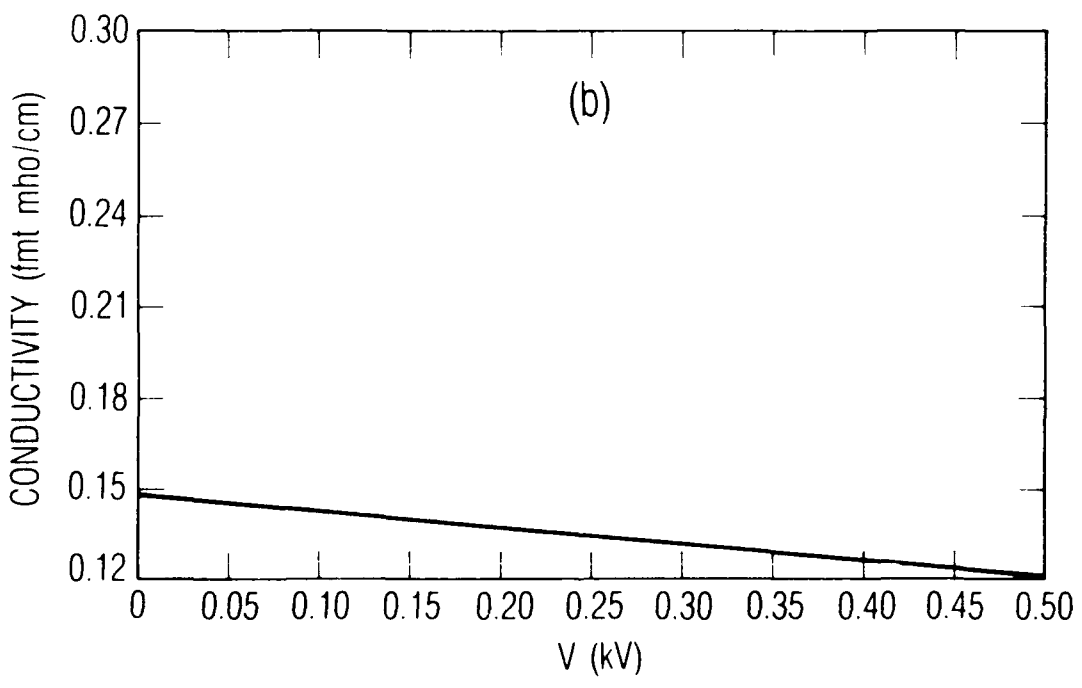
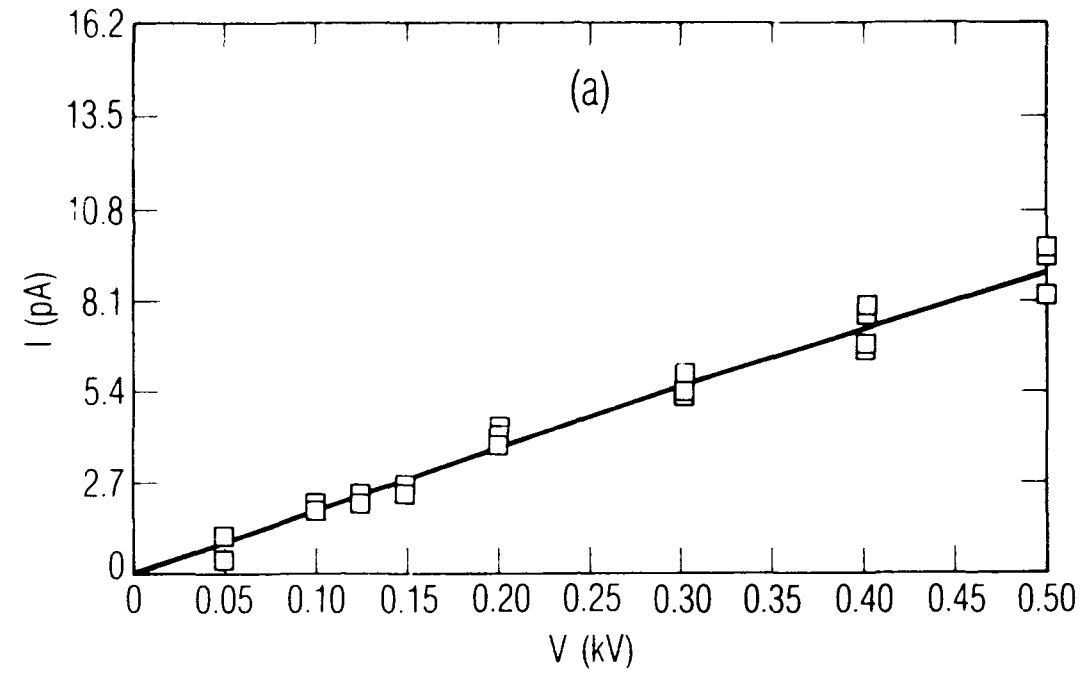


Fig. 3. (a) Current-voltage characteristic for unaged Uralane 5753, and (b) Conductivity (corresponding to Fig. 3a) for unaged Uralane 5753

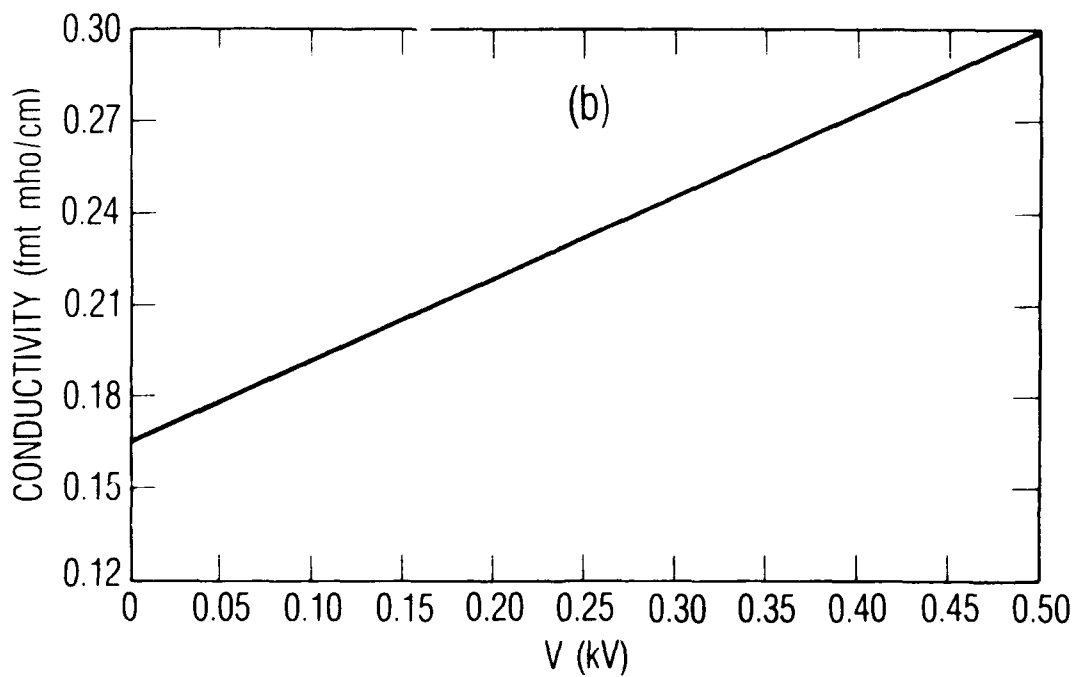
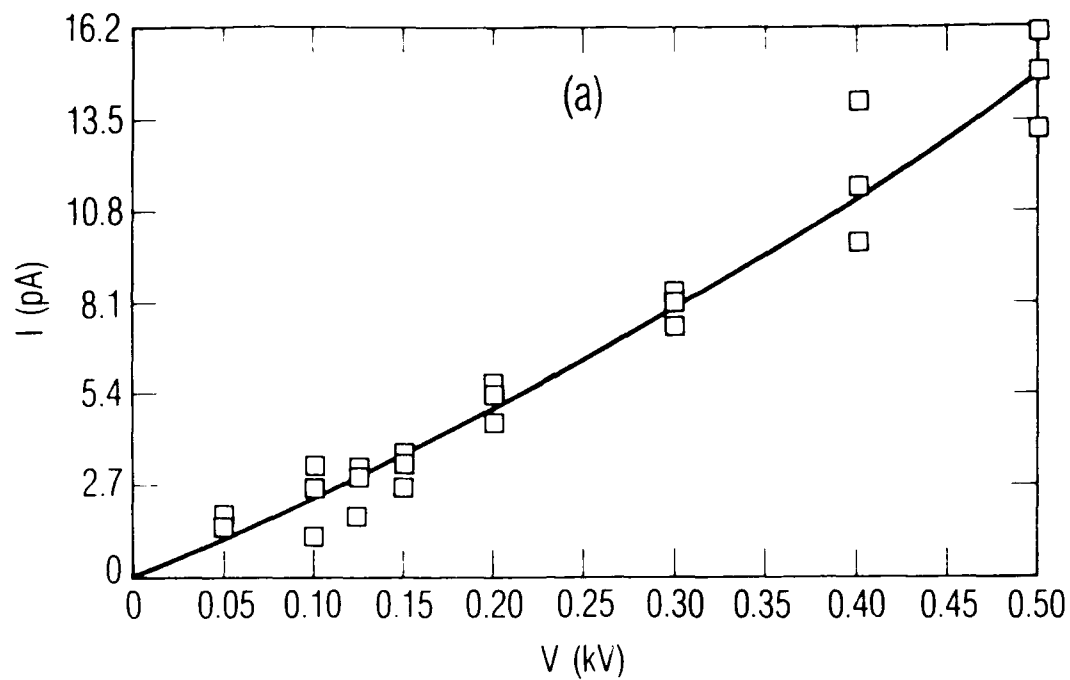


Fig. 4. (a) Current-voltage characteristic for Uralane 5753 aged for 0.5 hr at 120°C in air, and (b) Conductivity (corresponding to Fig. 4a) for Uralane 5753

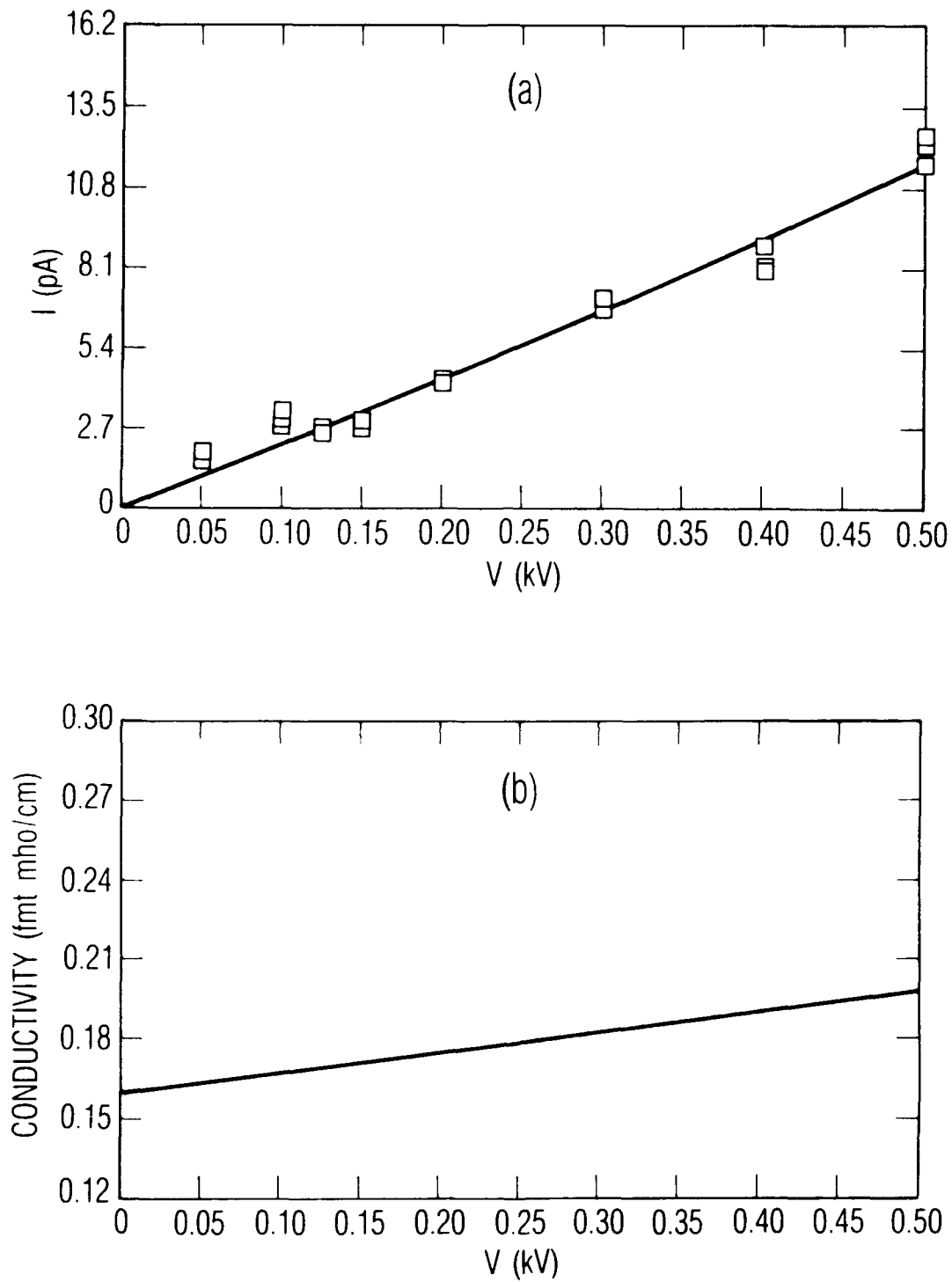


Fig. 5. (a) Current-voltage characteristic for Uralane 5753 aged for 4.0 hr at 120°C in air, and (b) Conductivity (corresponding to Fig. 5a) for Uralane 5753

Figure 6 shows the frequency-dependent permittivity (real part) for the initial material (top), the 0.5-hr aged sample (bottom), and the 4.0-hr aged sample (middle). The successive values at 1.0 kHz are 3.48, 3.09 (0.5 hr), and 3.27 (4.0 hr). The dielectric constant of the oil used in this two-fluid procedure was observed to be a flat function of frequency, with a value, 3.08, conforming to the value obtained in other experiments and supporting our confidence in the accuracy of these measurements. The linear response in the log-log plot was analyzed by least-squares curve fitting (solid lines in Fig. 6). The equation $\log(\text{real part of permittivity}) = a - b * \log(\text{frequency in kilohertz})$ has the following sets of parameters:

<u>Time</u>	<u>a</u>	<u>b</u>
0.0 hr	1.251	0.0279
0.5	1.131	0.0227
4.0	1.185	0.0272

This relaxation has been attributed to the microbrownian motion of the polybutadiene segments in a styrene-polybutadiene-styrene copolymer.² In Fig. 6 there is a distribution of relaxation times, because an attempt to fit the data with a single Debye relaxation was not successful.

Figures 7 and 8 show crossplots of the dc conductivity and the nominal dielectric breakdown strength, both plotted against the real part of the permittivity at 1.0 kHz. The dc conductivity is a decreasing function of the real part of the permittivity (Fig. 7), consistent with the working hypothesis. The more finely divided the dielectric, the more charge can be stored by interfacial polarization, affecting the permittivity via multipole interactions between the domains. Along with this, a more finely divided dielectric has more interfacial area with electron traps which decrease the conductivity. In Fig. 8, the average of six dielectric breakdown measurements is plotted along with the standard deviation. There is not much variation in the F_b value, compared with the measurement's standard deviation, but there is a small increase in F_b with increasing permit-

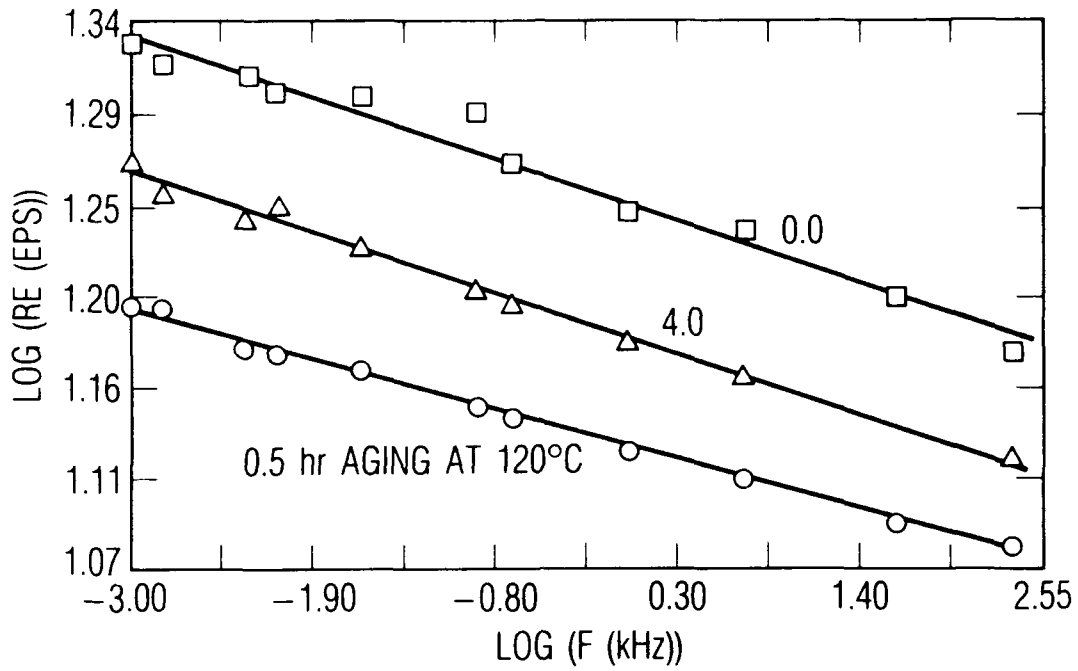


Fig. 6. Logarithm of the real part of the permittivity graphed against the logarithm of the frequency for unaged, 0.5-hr-aged, and 4.0-hr-aged Uralane 5753

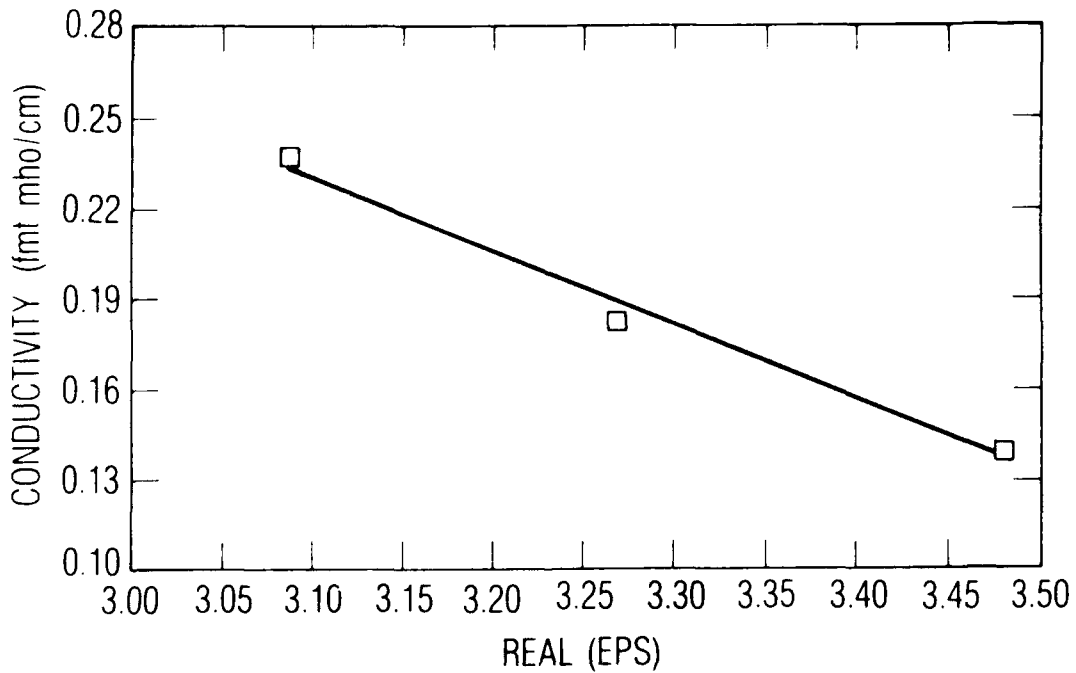


Fig. 7. Conductivity (at 250 V) of Uralane 5753 graphed against the real part of the permittivity at 1.0 kHz

tivity (Fig. 8), consistent with our basic hypothesis. We plan to implement the procedure for $F_b^{(o)}$ and expect to observe a stronger variation of $F_b^{(o)}$ with the permittivity.

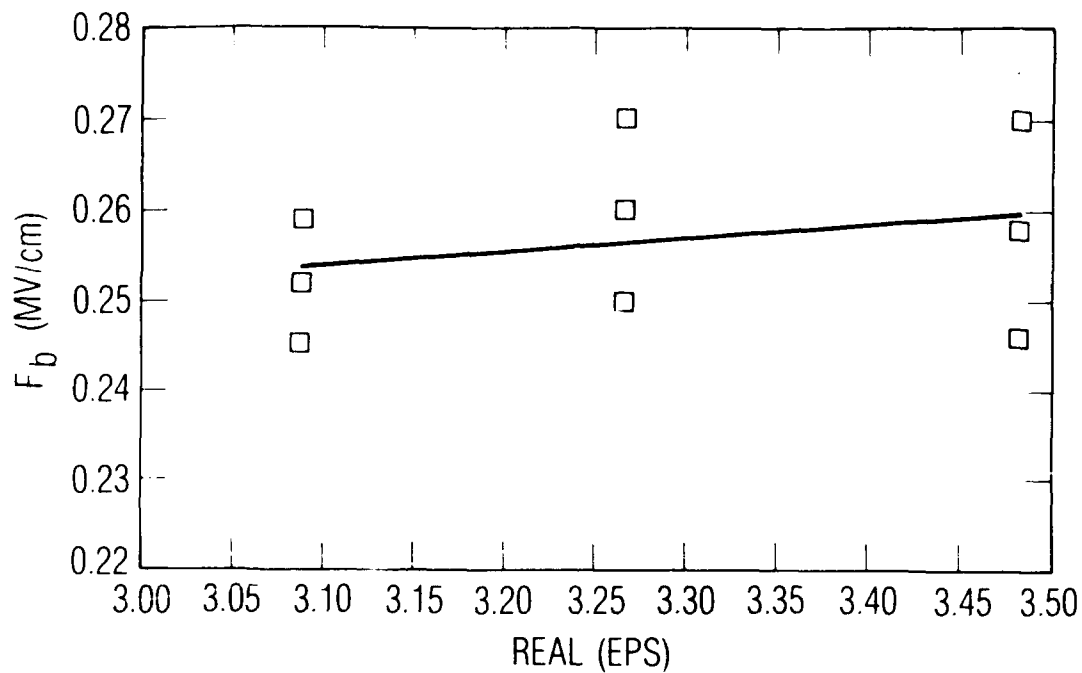


Fig. 8. Nominal dielectric breakdown strength of Uralane 5753 graphed against the real part of its permittivity at 1.0 kHz

IV. SUMMARY AND CONCLUSION

Structural irregularities in polymers lead to localized electron states (traps) and ultralow electron mobilities. Under high fields near electrode protrusions these traps can be ionized, and the mobility dramatically increases. The electric field near the protrusions is thereby limited, and space charge is injected into the polymer in order to satisfy the Laplace equation.⁹⁻¹³ Electron-phonon scattering limits the energy that the injected electrons can pick up. Nevertheless, at around 60% of the intrinsic transition (ionization) field (10 MV/cm), more than 1% of the injected electrons acquire energies above 1 eV, and electron impact ionization leads to tree formation and dielectric failure.¹⁰ The effect of hot (above 2.5 eV) electrons on organic dielectrics has been demonstrated.²⁹

The existence of phase separation and polymer microstructure with varying degrees of irregularity in some block copolymers is known to cause characteristic effects in dielectric relaxation spectra. We hypothesized that polyurethanes with phase-separated domains would also exhibit characteristic effects in the conductivity and permittivity. In addition, substantial effects of microstructure on F_b or $F_b^{(0)}$ were anticipated. We tested this hypothesis on the polyurethane, Uralane 5753. Thermal aging (0.0, 0.5, and 4.0 hr at 120°C) was used to vary the microstructure, as verified by FTIR. The changes were small, as verified by mechanical-property tests. The water content of the samples was less than or equal to 0.040% in all cases.

The working hypothesis found support in the correlation of the dc conductivity with the real part of the permittivity (Fig. 7). More finely subdivided (phase separated) polymers accumulate more charge due to the MWS effect. (The multipole interaction allows the permittivity to increase or decrease.) Traps at crystal/amorphous interfaces also reduce the conductivity in more highly phase-separated material. The correlation between F_b

and the real part of the permittivity was much less satisfying (Fig. 8), because F_b is not as good a measure of dielectric integrity as $F_b^{(0)}$. However, F_b did show a slight increase as the real part of the permittivity increased.

The conclusion is that small changes in domain characteristics lead to significant electrical effects, even in the absence of perceptible mechanical-property changes. More phase-separated materials draw less operating current and are therefore expected to be subjected to fewer energetic electrons which can potentially initiate failure during electrical aging.

REFERENCES

1. A. M. North, J. C. Reid, and J. B. Shortall, Eur. Polym. J. 5, 565 (1969).
2. A. M. North, R. A. Pethrick, and A. D. Wilson, Polymer 19, 913 and 923 (1978).
3. J. C. Maxwell, Treatise on Electricity and Magnetism, vol. 1, section 328-330, Oxford, Clarendon Press, London (1873).
4. K. W. Wagner, Arch. Elektotech. 2, 371 (1914).
5. R. W. Sillars, J. Instn. Elec. Engrs. 80, 378 (1937).
6. P. Fischer and P. Roehl, Prog. Colloid Poly. Sci. 62, 149 (1977).
7. P. Fischer, J. Electrostatics 4, 149 (1977/78).
8. R. M. Keyser, K. Tsuji, and F. Williams, "ESR and Optical Studies of Trapped Electrons in Glasses and Polymers," in Radiation Chemistry of Macromolecules, M. Dole, ed., Academic, NY (1972), Chap. 9, p. 145 (see especially p. 167).
9. H. R. Zeller and W. R. Schneider, J. Appl. Phys. 56, 455 (1984).
10. H. R. Zeller, P. Pfluger, and J. Bernasconi, IEEE Trans. Elec. Insul. EI-19, 200 (1984).
11. T. Hibma and H. R. Zeller, J. Appl. Phys. 59, 1614 (1986).
12. H. J. Wiesmann and H. R. Zeller, J. Appl. Phys. 60, 1770 (1986).
13. H. R. Zeller, IEEE Elec. Insul. EI-22, 115 (1987).
14. M. M. Z. Kharadly and W. J. Jackson, Proc. IEE 100, 199 (1953).
15. J. S. Dryden and R. J. Meakins, Proc. Phys. Soc. B70, 427 (1957).
16. R. S. Bretzlaff and T. B. Bahder, Rev. Phys. Appl. 21, 833 (1986).
17. R. S. Bretzlaff and S. L. Sandlin, FTIR Study of Thermal and Electrical Aging in Polyurethane, TR-0086(6925-08)-4, The Aerospace Corporation, El Segundo, CA (20 March 1987).
18. R. S. Bretzlaff, S. L. Sandlin, and M. A. Yasumatsu, Proceedings, First International SAMPE Electronics Conference, 23-25 June 1987, pp. 9-17.

19. R. S. Bretzlaff, T. B. Bahder and S. L. Sandlin, Prebreakdown Phenomena in Electrically Aged Polymeric Insulation, ATR 86(8480)-1, The Aerospace Corporation, El Segundo, CA (25 November 1986).
20. H. S. Endicott and E. J. McGowan, Conference on Elec. Insul., NAS-NAC, 1960 Annual Report, p. 19.
21. H. S. Endicott and W. E. Springgate, Conference on Elec. Insul., NAS-NAC, 1950 Annual Report, p. 43.
22. AC Loss and Permittivity of Solid Elec. Insul. Materials, ASTM D-150-81 (vol. 35).
23. A. E. W. Austen and H. Pelzer, Proc. IEE 93, 525 (1946).
24. W. G. Oakes, Proc. IEE 95, 36 (1948); 96, 37 (1949).
25. D. W. Bird and H. Pelzer, Proc. IEE 96, 44 (1949).
26. J. J. McKeown, Proc. IEE 112, 824 (1965).
27. P. Fischer and K. W. Nissen, IEEE Trans. Elec. Insul EI-11, 37 (1976).
28. P. Fischer and R. Roehl, Siemens Forsch.-u. Entwickl.-Bericht, 3, 125 (1974).
29. E. Cartier and P. Pfluger, IEEE Trans. Elec. Insul. EI-22, 123 (1987).

LABORATORY OPERATIONS

The Aerospace Corporation functions as an "architect-engineer" for national security projects, specializing in advanced military space systems. Providing research support, the corporation's Laboratory Operations conducts experimental and theoretical investigations that focus on the application of scientific and technical advances to such systems. Vital to the success of these investigations is the technical staff's wide-ranging expertise and its ability to stay current with new developments. This expertise is enhanced by a research program aimed at dealing with the many problems associated with rapidly evolving space systems. Contributing their capabilities to the research effort are these individual laboratories:

Aerophysics Laboratory: Launch vehicle and reentry fluid mechanics, heat transfer and flight dynamics; chemical and electric propulsion, propellant chemistry, chemical dynamics, environmental chemistry, trace detection; spacecraft structural mechanics, contamination, thermal and structural control; high temperature thermomechanics, gas kinetics and radiation; cw and pulsed chemical and excimer laser development, including chemical kinetics, spectroscopy, optical resonators, beam control, atmospheric propagation, laser effects and countermeasures.

Chemistry and Physics Laboratory: Atmospheric chemical reactions, atmospheric optics, light scattering, state-specific chemical reactions and radiative signatures of missile plumes, sensor out-of-field-of-view rejection, applied laser spectroscopy, laser chemistry, laser optoelectronics, solar cell physics, battery electrochemistry, space vacuum and radiation effects on materials, lubrication and surface phenomena, thermionic emission, photosensitive materials and detectors, atomic frequency standards, and environmental chemistry.

Electronics Research Laboratory: Microelectronics, solid-state device physics, compound semiconductors, radiation hardening; electro-optics, quantum electronics, solid-state lasers, optical propagation and communications; microwave semiconductor devices, microwave/millimeter wave measurements, diagnostics and radiometry, microwave/millimeter wave thermionic devices; atomic time and frequency standards; antennas, rf systems, electromagnetic propagation phenomena, space communication systems.

Materials Sciences Laboratory: Development of new materials: metals, alloys, ceramics, polymers and their composites, and new forms of carbon; nondestructive evaluation, component failure analysis and reliability; fracture mechanics and stress corrosion; analysis and evaluation of materials at cryogenic and elevated temperatures as well as in space and enemy-induced environments.

Space Sciences Laboratory: Magnetospheric, auroral and cosmic ray physics, wave-particle interactions, magnetospheric plasma waves; atmospheric and ionospheric physics, density and composition of the upper atmosphere, remote sensing using atmospheric radiation; solar physics, infrared astronomy, infrared signature analysis; effects of solar activity, magnetic storms and nuclear explosions on the earth's atmosphere, ionosphere and magnetosphere; effects of electromagnetic and particulate radiations on space systems; space instrumentation.